Uniform Circular Arrays: the Key to Optimum Channel Capacity in Mobile MIMO Satellite Links

V. Dantona[1)], R.T. Schwarz[2)], A. Knopp[2)] and B. Lankl[1)]
Email: {vito.dantona, robert.schwarz, andreas.knopp, berthold.lankl}@unibw.de

[1)] Institute for Communications Engineering
Munich University of the German Bundeswehr
85579 Neubiberg, Germany

[2)] Federal Office of the German Armed Forces (Bundeswehr)
for Information Management and Information Technology
Satellite Communications Division, 56026 Koblenz, Germany

***Abstract*—In this paper, we investigate the benefits of uniform circular arrays (UCAs) as an alternative antenna deployment to uniform linear arrays (ULA), which are commonly applied for multiple-input multiple-output (MIMO) systems. We consider a MIMO satellite link with focus on the Line-of-Sight (LOS) signal component of the MIMO channel between two geostationary satellites and a mobile earth terminal equipped with several antennae. The MIMO LOS channel is optimized with respect to the maximum achievable spectral efficiency. The aim of our approach is to keep this optimum spectral efficiency nearly constantly even if the terminal on earth is moving. We provide an analytical derivation for the optimum UCA arrangement and prove our results by numerical simulations. Especially for mobile applications, the UCA antenna arrangement seems to be a reasonable candidate in order to guarantee high capacity performance durably. To this end, we present a very simple triangle shaped antenna arrangement which is compact enough to allow vehicle roof top installations for S-band applications.**

I. Introduction

Multiple-Input Multiple-Output (MIMO) systems have recently attracted increasing attention because of the potential increase of the bandwidth efficiency compared to commonly known Single-Input Single-Output (SISO) systems [1], [2]. Since a linear increase of the spectral efficiency can be achieved in a MIMO system with the number of antenna elements at the receiver and the transmitter, these multi-antennae systems are especially promising in satellite communications systems, as the available frequency bandwidth is a scarce transmission resource [3].

Of course, the typical satellite channel is mainly characterized by a strong Line-of-Sight (LOS) signal component in nearly all application cases, rather than a rich scattering environment. Although numerous publications demand various uncorrelated multipath signal components at the receiver end in order to achieve the theoretical MIMO multiplexing gain, it has been shown that even pure LOS MIMO channels can be optimized with respect to the maximum possible spectral efficiency [4]. Actually, the authors in [5] presented a strategy to optimize the spectral efficiency of MIMO satellite links between two antennae in the geostationary orbit and several antennae on earth all arranged within a uniform linear array (ULA), both for regenerative and transparent payloads.Other previous works focused on the effects of satellite station-keeping maneuvers [6] and atmospheric impairments [7] on the MIMO link. Although this approach meets the high capacity requirements for fixed satellite services very well, the use of ULAs provides some disadvantages in the case of mobile satellite applications as the spectral efficiency can collapse to its minimum value (keyhole-channel) because of the mobility of the ground terminal.

In order to overcome this drawback of ULAs in mobile scenarios, in this paper we present the uniform circular array (UCA) as an alternative antenna configuration at the ground terminal side, using [5] as a starting point. UCAs have been often proposed in the literature for MIMO systems, even in LOS scenarios [8], [9], but their possible application to SatCom was so far quite unexplored.

After introducing the system model and the derivation of the spectral efficiency in Section II, we will derive in Section III an analytical model for the geometrical UCA parameters ensuring optimum spectral efficiency even if the terminal on earth is moving. We will prove the feasibility of ring-like antennae structures for mobile terminals through numerical simulation results in Section IV, and we will conclude with Section V.

II. MIMO Spectral Efficiency and System Model

A. Channel Model

The MIMO channel can be described through a channel transfer matrix $\mathbf{H}(f)$, which contains the channel transfer function for each pair of antennae at transmitter and receiver. The channel transfer matrix may be split into a Line-Of-Sight (LOS) component $\mathbf{H}_{LOS}(f)$, which models the free-space signal propagation, and a second component $\mathbf{H}_{NLOS}(f)$ collecting all multipath contributions. Altough a strong LOS component would be desired for any satellite applications, shadowing and blocking, which mainly occurr in urban environments, cannot be avoided in the Land Mobile Satellite (LMS) channel, so that the NLOS component arising from multipath propagation cannot be in principle ignored. Nevertheless, an antenna separation of at least half wavelength λ is commonly assumed in pure NLOS environments [10]. Therefore, we restrict ourselves in this paper to find a geometrical criterion for the antenna setup optimization in LOS conditions and we assume that this is anyway not detrimental for the NLOS component, as long as the $\lambda/2$-criterion is not infringed. A more exact evaluation, including the definition of

an appropriate MIMO LMS channel model, is left for future work.

We assume in the following a frequency flat MIMO LOS channel $\mathbf{H}(f) = \mathbf{H}_{LOS}$, where the carrier frequency f_c is much higher than the system bandwidth B, i.e. $f_c \gg B$.

Under these assumptions, if we consider a general system with M_T transmitting satellite antennae and M_R receiving antennae at ground terminal, the channel transfer matrix entries due to free space propagation may be expressed as

$$H_{m_R,m_T} = a_{m_R,m_T} \cdot \exp\left\{-j\frac{2\pi f_c}{c_0} r_{m_R,m_T}\right\}, \qquad (1)$$

with c_0 being the speed of light in free space and r_{m_R,m_T} being the distance from the m_R-th ground antenna to the m_T-th satellite antenna, for $m_T = 1,\ldots,M_T$ and $m_R = 1,\ldots,M_R$. The term $a_{m_R,m_T} = \frac{c_0}{4\pi f_c r_{m_R,m_T}} \mathrm{e}^{j\phi}$ is the complex envelope, for which $\phi = 0$ will be assumed in the following, as it is a phase angle common to all channel matrix entries. Moreover, we assume $a_{m_R,m_T} \approx |a|$, i.e. the magnitude of the channel gain is approximately constant for each couple of Tx and Rx antennae, as the distance from the ground station to the satellites is much larger than the array sizes.

B. MIMO Spectral Efficiency

The channel transfer matrix impacts the achievable spectral efficiency according to the equation [1]

$$C = \log_2\left[\det\left(\mathbf{I}_{M_R} + \rho \cdot \mathbf{H}\mathbf{H}^H\right)\right], \qquad (2)$$

where the transmit symbols are realizations of uncorrelated, independent identically distributed (i.i.d.) gaussian random variables. The linear transmit signal-to-noise ratio ρ is defined as the carrier-to-noise ratio $\mathcal{C}/\mathcal{N}_0^{\text{down.}}$ as seen from the receiver without the path-loss

$$\rho = \mathcal{C}/\mathcal{N}_0^{\text{down.}} + L_{FS} = \mathit{EIRP}_{\text{Tx}} + (G{-}T)_{\text{Rx}} - \mathcal{K} \qquad (3)$$

where $\mathit{EIRP}_{\text{Tx}}$ is the equivalent isotropic radiated power per satellite antenna, $(G{-}T)_{\text{Rx}}$ is the figure-of-merit of the receive terminal per receive antenna and $\mathcal{K} = 10 \cdot \log_{10}(k_B) = -228,6\,\text{dBWs/K}$ is the logarithmic value of the Boltzmann constant k_B. It is assumed here that ρ is constant and identical for each pair of Tx-Rx antennae, and that this ratio includes all the gains of the link budget, except for the LOS path loss, which has been incorporated into the channel matrix through the term a_{m_R,m_T} of equation (1).

Let the square matrix $\mathbf{V}$ with eigenvalues γ_i be defined as follows:

$$\mathbf{V} = \begin{cases} \mathbf{H}^H\mathbf{H} & M_R \geq M_T \\ \mathbf{H}\mathbf{H}^H & M_R < M_T \end{cases}, \qquad (4)$$

and let $M_{\min} = \min\{M_T, M_R\}$ and $M_{\max} = \max\{M_R, M_T\}$. The maximum spectral efficiency is achieved when all eigenvalues of $\mathbf{V}$ are identical, i.e. $\gamma_i = |a|^2 M_{\max}$ for $i = 1,\ldots,M_{\min}$. If this condition is satisfied, the value of the spectral efficiency becomes

$$C_{\text{opt}} = M_{\min} \cdot \log_2\left(1 + \rho|a|^2 M_{\max}\right), \qquad (5)$$

which is the upper bound we aim to achieve in the following.

On the contrary, the lower bound for the spectral efficiency is achieved if the channel matrix becomes rank-deficient and the so-called *keyhole effect* occurs.

The aim of the geometrical spectral efficiency optimization is to adjust the channel matrix entries so that the eigenvalues of $\mathbf{V}$ are equal, and $M_{\min}$ identical eigenmodes are thus generated. As shown in equation (1), the path lengths between each couple of Tx and Rx antennae are the degrees of freedom which can be exploited for this purpose.

C. System Parameters and Scenario Description

In our investigations we consider a downlink scenario between $M_T = 2$ transmit antennae placed on two distinct satellites in the geostationary orbit and a mobile receiver endowed with an arbitrary number of M_R receive antennae. Therefore, the resulting MIMO satellite channel is of the order $M_R \times 2$. As the present approach is particularly focused on mobile scenarios we assume a carrier frequency within the S-frequency band of $f_c = 2.2\,\text{GHz}$ (typically used especially in mobile satellite applications, e.g. [11]). The considered link-budget for our investigations is according to table I, where $L_{FS} = -20\,\log_{10}(|a|) \approx 190\,\text{dB}$ is the free-space path loss at $2.2\,\text{GHz}$ for an average transmission path length between a geostationary satellite and a ground receiver.

It is important to note, that we assume that both satellites have identical transmission characteristics and, furthermore, are synchronized for example through an inter satellite link [3].

carrier frequency	$f_c = 2.2\,\text{GHz}$ (S-Band)
satellite antenna gain	$G_T = 30\,\text{dBi}$
satellite power (at antenna feed)	$P_T = 17\,\text{dBW}$
resulting EIRP	$\mathit{EIRP}_{\text{Tx}} = 47\,\text{dBW}$
Rx antenna gain	$G_R = 8\,\text{dBi}$
Rx system noise temperature	$T = 140\,\text{K}$
resulting G/T	$(G{-}T)_{\text{Rx}} = -13,8\,\text{dB/K}$
free space path loss	$L_{FS} = 190\,\text{dB}$
carrier-to-noise ratio at Rx	$\mathcal{C}/\mathcal{N}_0^{\text{down.}} = 71,8\,\text{dBHz}$

TABLE I
CHARACTERISTICS OF THE SATELLITE SYSTEM

III. CAPACITY-OPTIMUM UCAS

A. Background and Motivation

In [5], a method was presented for optimizing the spectral efficiency of the MIMO channel illustrated in Section II-C. In that case, the ground receiver was equipped with a ULA, as shown in Figure 1. The geometrical parameters of interest were the antenna separation d and the array orientation angle δ, measured with respect to the geographical east-west direction. A condition on these two parameters was derived, which ensured the achievement of the optimal spectral efficiency.

Nevertheless, the obtained results were not suited for mobile applications. Whereas the antenna separation may be thought as a fixed parameter and it can thus be optimized once for all, in a mobile scenario the ground receiver will continuously

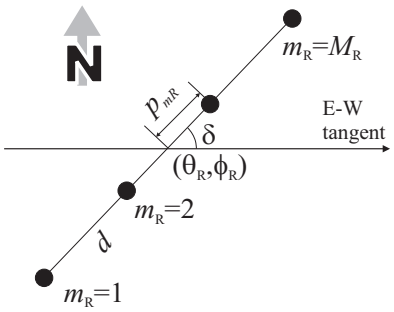

Fig. 1. Top view of the ground terminal ULA deployment for $M_R = 4$

change its orientation angle, and thus the achievement of the optimal spectral efficiency would not be guaranteed any more. Actually, for any given value of antenna separation, there are at least two "critical" values of δ, for which the spectral efficiency even degrades to the keyhole value (Figure 2).

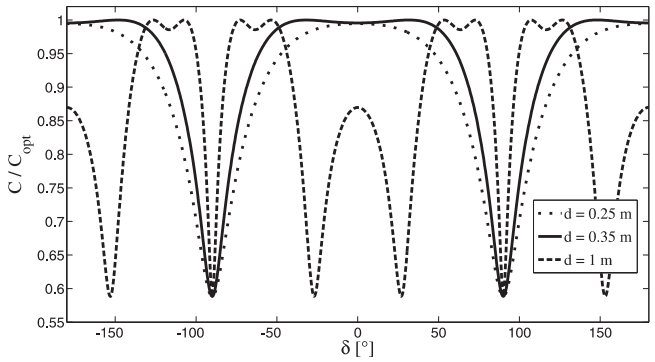

Fig. 2. Spectral efficiency with a ULA receiver as a function of the array orientation angle δ for different values of the antenna separation d, derived exemplarily from [5]

For this reason, it is desirable to investigate alternative antenna deployments which could improve the robustness of the MIMO system as the receiver changes its position. In the previous work, it was already suggested that a ring-like antenna structure could be a significant choice and some antenna setups were qualitatively proposed. In this section we are going to derive a geometrical model for the spectral efficiency optimization of the simplest possible ring-like structure, i.e. the uniform circular array.

B. Geometrical Description

The positions of the ground terminal and of the satellites are described by the notation introduced in Figure 3. The center of the ground terminal has latitude ϕ_R and longitude θ_R on the Earth surface, while the position of each satellite is described by the single angle θ_{T,m_T}, with $m_T = 1, 2$, due to the geostationary orbit. R_E and R_G denote the mean Earth radius and the radius of the geostationary orbit, respectively.

The cartesian coordinates of the m_T-th satellite are therefore:

$$\begin{pmatrix} x_{m_T} = R_G \cos\theta_{T,m_T} \\ y_{m_T} = R_G \sin\theta_{T,m_T} \\ z_{m_T} = 0 \end{pmatrix}, \tag{6}$$

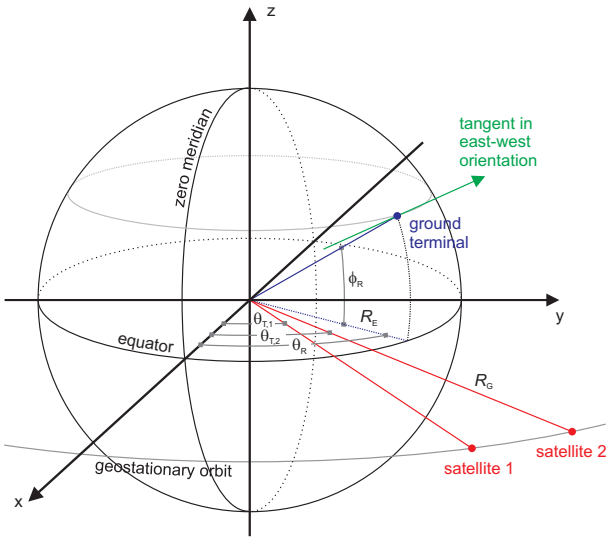

Fig. 3. Scenario and Coordinate System

while for the center of the ground terminal we may define:

$$\begin{pmatrix} x_R = R_E \cos\phi_R \cos\theta_R \\ y_R = R_E \cos\phi_R \sin\theta_R \\ z_R = R_E \sin\phi_R \end{pmatrix}. \tag{7}$$

So far, the antenna displacement at the ground terminal was not yet considered. This displacement is modeled as shown in Figure 4. It is assumed that the antenna array lies on a plane tangential to the Earth's surface. The antenna elements are equally spaced on a virtual circumference of diameter D. One antenna element is identified as reference by the index $m_R = 1$ and the other elements are numbered by increasing m_R in counterclockwise direction. Without loss of generality, we define also for the UCA the *array orientation angle* δ, as it was done for the ULA. More exactly, δ is defined in this case as the angle formed by the ideal tangent to the Earth running in the east-west direction and the UCA radius having the antenna element denoted by $m_R = 1$ as endpoint. The array orientation angle may thus be thought as an offset rotation applied to the whole array, and would continuously change as a mobile terminal moves. For this reason, it is clearly a critical parameter which has to be accounted for in the design and optimization of the mobile terminal.

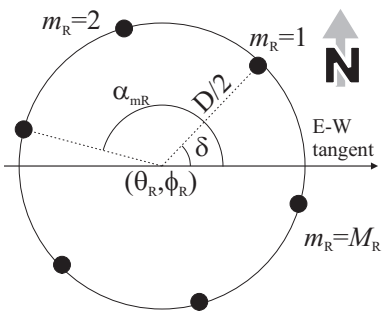

Fig. 4. Top view of the ground terminal UCA deployment for $M_R = 6$

For each antenna element m_R it is straightforward to define the angle formed by the UCA radius terminating on that element and the east-west tangent as:

$$\alpha_{m_R} = \frac{2\pi}{M_R}(m_R - 1) + \delta. \tag{8}$$

That allows to derive a general expression for the cartesian coordinates of each single antenna element as $(x_{m_R}, y_{m_R}, z_{m_R})^T =$

$$\begin{pmatrix} x_R - \frac{D}{2}\left(\sin\theta_R \cos\alpha_{m_R} + \sin\phi_R \cos\theta_R \sin\alpha_{m_R}\right) \\ y_R + \frac{D}{2}\left(\cos\theta_R \cos\alpha_{m_R} - \sin\phi_R \sin\theta_R \sin\alpha_{m_R}\right) \\ z_R + \frac{D}{2}\cos\theta_R \sin\alpha_{m_R} \end{pmatrix}. \tag{9}$$

The distance of each antenna element from the center of the array is obviously independent of m_R and equal to $D/2$, while the angular separation grows linearly with m_R. It may be worth noting that this situation is exactly the opposite of the one encountered in the ULA-case, where all vectors from each antenna elements to the center had the same angle δ, but linearly increasing length $p_{m_R} = \left(m_R - 1 - \frac{M_R - 1}{2}\right) d$, with d being the uniform antenna spacing. The ULA antenna configuration was given for reference in Figure 1.

It is worth noting again that the proposed geometrical description assumes that the UCA plane is always tangential to the Earth's surface, since the array orientation is described through a single angle δ. This simplification was introduced because it is reasonable to think about roof top installations of the antenna array on buildings or vehicles. Of course, there may be some specific applications not covered by this work (e.g. vehicles climbing on very steep paths) where the elevation angle might also play a significant role.

C. General Optimization Criterion

As explained in [2], there is in general a link between the geometrical displacement of the antennae and the spectral efficiency in presence of a LOS channel. Thanks to the approximation on the magnitude of the channel gains introduced in Section II-A, equation (1) actually shows that the phase relations between the channel matrix entries are the only degrees of freedom on which one could act in order to modify the properties of the channel. A criterion on these phase relations which allows to maximize the spectral efficiency for a $M_R \times 2$ MIMO channel was derived in [5], by imposing the eigenvalues of $\mathbf{H}^H\mathbf{H}$ to be equal, as explained in Section II-B. The most general formulation of this criterion, which can be used as a starting point for the present work, can be expressed as follows:

$$r_{k,1} - r_{k,2} + r_{l,2} - r_{l,1} = v\,(k - l)\,\frac{c_0}{M_R f}, \tag{10}$$

where r_{m_R,m_T} is the path length from the m_T-th transmit antenna to the m_R-th receive antenna. This equation gives for each couple of receive antenna elements $k, l = 1, \ldots, M_R$ the condition that leads the channel matrix to have identical eigenmodes and thus maximizes the spectral efficiency. Here the parameter $v \in \mathbb{Z}$, indivisible by M_R has been introduced, since the possible configurations which satisfy the condition have actually an angle periodicity of 2π.

D. Optimizing the UCA Antenna Arrangement

In this paper, we aim at applying the condition (10) to a UCA. So, the equation should be reformulated, in order to keep into account the peculiarities of the circular antenna deployment.

First of all, in a circular array the distance between two antenna element indices a and b may always be cyclically normalized within the range $\left[\lceil -\frac{M_R}{2} \rceil, \lceil \frac{M_R}{2} - 1 \rceil\right]$. For this purpose, we define the following operator:

$$a \ominus b \triangleq \begin{cases} a - b & \mid a - b \mid \leq \frac{M_R}{2} \\ a - b - M_R \cdot \mathrm{sign}(a - b) & \mid a - b \mid > \frac{M_R}{2} \end{cases}. \tag{11}$$

We will therefore replace $(k - l)$ in (10) with $(k \ominus l)$:

$$r_{k,1} - r_{k-2} + r_{l,2} - r_{l,1} = v\,(k \ominus l)\,\frac{c_0}{M_R f}. \tag{12}$$

As a second step, we look for an expression of the path lengths r_{m_R,m_T} which depends on the geometrical parameters introduced in Section III-B. Generally speaking, the path length may be obviously expressed as the Euclidean norm of the distance vector between an antenna element m_R at ground terminal and an antenna element m_T in orbit, i.e. following the notation introduced previously:

$$r_{m_R,m_T} = \sqrt{\left(x_{m_R} - x_{m_T}\right)^2 + \left(y_{m_R} - y_{m_T}\right)^2 + z_{m_R}^2}, \tag{13}$$

where we have already taken into account that $z_{m_T} = 0$ for geostationary satellites.

Applying eq. (6) and (9) we obtain for the path length

$$\begin{aligned} r_{m_R,m_T} \;=\; & \Big\{ R_G^2 + R_E^2 - 2R_G R_E \cos\phi_R \cos\Delta\theta_{m_T} \\ & + DR_G \left[\cos\alpha_{m_R} \sin\Delta\theta_{m_T} \right. \\ & \left. + \sin\alpha_{m_R} \cos\Delta\theta_{m_T} \sin\phi_R\right] + \frac{D^2}{4} \Big\}^{\frac{1}{2}} \end{aligned} \tag{14}$$

where the following substitution is used for ease of notation:

$$\Delta\theta_{m_T} = \theta_R - \theta_{T,m_T}. \tag{15}$$

Analogously as in the ULA case, two auxiliary quantities are now introduced:

$$s_{m_T} \;=\; \left[R_G^2 + R_E^2 - 2R_E R_G \cos\phi_R \cos\Delta\theta_{m_T}\right]^{\frac{1}{2}} \tag{16}$$

$$\begin{aligned} c_{m_R,m_T} \;=\; & 2R_G \left[\cos\alpha_{m_R} \sin\Delta\theta_{m_T} \right. \\ & \left. + \sin\alpha_{m_R} \cos\Delta\theta_{m_T} \sin\phi_R\right]. \end{aligned} \tag{17}$$

Whereas s_{m_T} keeps exactly the same meaning as for ULAs[1], the second parameter is now also dependent on m_R, and no more only on m_T.

At this stage, the approximation of the square root $\sqrt{1 + \Delta} \approx 1 + \frac{\Delta}{2}$ can be applied. These considerations lead

[1]The parameter s_{m_T} may be geometrically interpreted as the distance between the m_T-th satellite antenna and the center of the ground terminal array.

to the following expression of the path lengths:

$$r_{m_R,m_T} = \sqrt{s_{m_T}^2 + \frac{D}{2}\, c_{m_R,m_T} + \frac{D^2}{4}} \quad (18)$$

$$\approx s_{m_T} + \frac{D}{4}\frac{c_{m_R,m_T}}{s_{m_T}}. \quad (19)$$

This result may now be inserted into (12) and the resulting equation is

$$\frac{D}{4}\left(\frac{c_{k,1}+c_{l,1}}{s_1} - \frac{c_{k,2}+c_{l,2}}{s_2}\right) = v\,(k \ominus l)\,\frac{c_0}{M_R f}. \quad (20)$$

A comparison with the result obtained for ULAs clearly shows that this time the optimization criterion keeps the dependence on the difference between k and l (actually on its normalized form $k \ominus l$). In the ULA case, this dependence disappeared thanks to the linear nature of the array structure and the optimization of the array geometry became independent of a particular choice of k and l. In the UCA case on the contrary, the term $(k \ominus l)$ shows that different solutions exist, according to the particular couple of antenna elements which is considered for the optimization. In other words, each couple (k, l) of antennae may be seen as a 2-elements ULA, and optimizing the UCA geometry is equivalent to the joint optimization of these $M_R^2 - M_R$ ULAs which compose the circular array. In the next section, we will try to simplify eq. (20) in order to highlight how it is related to the geometrical setup of the receiver array.

E. UCA Optimization Criterion

As it was shown in Figure 4, the degrees of freedom in the design of the UCA are:

- the number of antennae M_R;
- the array diameter D;
- the array orientation δ.

Assuming that M_R is given, we aim at finding the values of D and δ which maximize the spectral efficiency. For this reason, it is necessary to reformulate equation (20) in order to make the dependency on these two optimization parameters explicit. Whereas the dependency on D is already evident, it is also possible to manipulate the sums $c_{k,m_T} + c_{l,m_T}$ by applying some trigonometrical theorems and get:

$$(c_{k,m_T} + c_{l,m_T}) = R_G\left(G_{kl,m_T}^{(C)}\cos\delta + G_{kl,m_T}^{(S)}\sin\delta\right). \quad (21)$$

The coefficients $G_{kl,m_T}^{(C)}$ and $G_{kl,m_T}^{(S)}$ include all parameters related to the receiver and satellites positions, but independent of the optimization parameters. Their full expression is given in the Appendix. The result of (21) may be now inserted into (20), after assuming the following definitions for ease of notation:

$$A_{kl} = \frac{G_{kl,1}^{(C)}}{s_1} - \frac{G_{kl,2}^{(C)}}{s_2} \quad (22)$$

$$B_{kl} = \frac{G_{kl,1}^{(S)}}{s_1} - \frac{G_{kl,2}^{(S)}}{s_2} \quad (23)$$

$$Q_{kl} = \frac{4\,(k \ominus l)\,c_0}{R_G M_R f} \quad (24)$$

The optimization equation thus becomes

$$D\,(A_{kl}\cos\delta + B_{kl}\sin\delta) = v_{kl}\cdot Q_{kl}. \quad (25)$$

As we have one equation for each couple (k, l) with $k \neq l$, equation (25) actually describes a non-linear system of $M_R^2 - M_R$ equations in the variables D and δ. Moreover, the parameter v_{kl} represents a further degree of freedom for *each* equation of the system. As we are dealing with an overdetermined system, we can assume that *appoximate* solutions may be found in the Least Squares sense, but it is obviously impossible to give a closed-form expression for an *exact* solution of the system, and thus for the values of D and δ which would ensure full achievement of the optimal spectral efficiency. For this reason, we continue our analysis through numerical simulations, which we will show in the following section.

IV. Numerical Simulations and Interpretation

A. Numerical Evaluation of the Spectral Efficiency

A basic simulator has been implemented, which can numerically compute the LOS channel matrix, and thus the spectral efficiency, for a given geometrical arrangement of the transmitting satellites and of the receiver antennae. These numerical simulations have two main purposes:

- verify whether the UCA antenna deployment would offer a better robustness against movements of the receiver, if compared with a ULA;
- verify whether there exist some UCA configurations which allow to achieve 100% of the optimum spectral efficiency, although the equation system (25) does not allow a closed-form solution.

Figure 5 displays the contour plot of the calculated spectral efficiency as a function of D and δ, assuming a 3-element UCA at the receiver. For this example the satellites were situated at the geographical positions of 9° and 17° East, respectively (similar results can be obtained for any mutual positions of satellites and receiver, as long as the visibility is ensured). It is quite evident that *a near-maximum spectral efficiency is achievable in the white zone independently of the array orientation*, by choosing values of D in the range between approximately 50 and 70 cm. Within the marked range, the spectral efficiency is bounded between 98% and 100% of the optimum value. Moreover, the plot clearly shows six keyholes which arise at about $D = 1.2\,\mathrm{m}$ for $\delta = n \cdot 60°$, $n = 0, \ldots, 5$, as well as the obvious drop of the spectral efficiency for $D = 0$. These first statements already seem to validate the initial hypothesis on the robustness of the UCA architecture against variations of the orientation angle δ. It must be noted, that these results are dependent on the satellite displacement which was set to 8° in this example. In general, the optimum range of 50 to 70 cm becomes larger for smaller satellite separations and vice-versa [5].

We observe now that equation (25) describes a straight line on the cartesian plane $(D\cos\delta, D\sin\delta)$, whose slope depends on the parameters A_{kl} and B_{kl}. It looks therefore

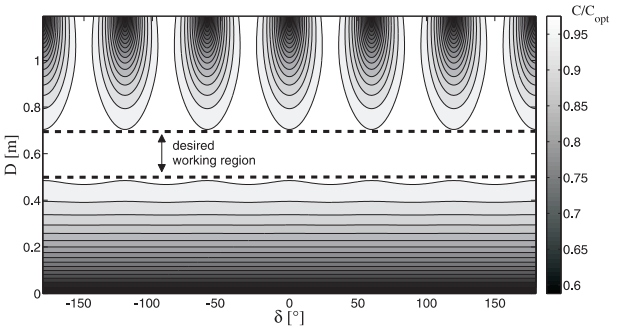

Fig. 5. Spectral Efficiency computed by numerical simulations for $M_R = 3$, $\rho = 203\,\mathrm{dB}$, $\theta_R = 13°, \phi_R = 52°$ and $\theta_{T,1/2} = 13° \pm 4°$.

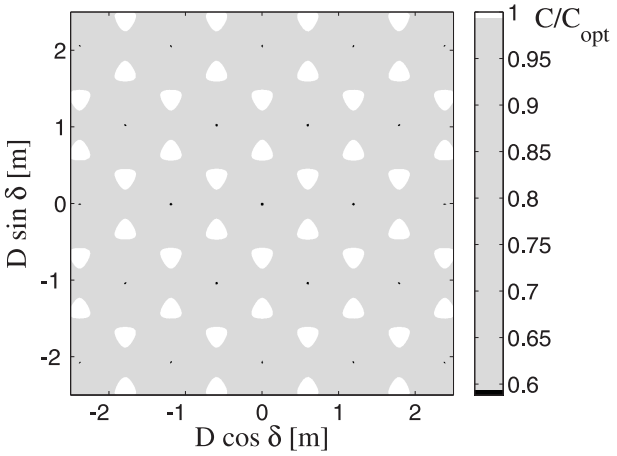

Fig. 6. Polar coordinates representation of the spectral efficiency computed by numerical simulations for $M_R = 3$, $\rho = 203\,\mathrm{dB}$, $\theta_R = 13°, \phi_R = 52°$ and $\theta_{T,1/2} = 13° \pm 4°$.

reasonable to transform the spectral efficiency plot of Figure 5 into this modified coordinate system. This is shown in Figure 6, where the color scale has been compressed in order to enhance the optimum spectral efficiency values (in white) and the keyholes (in black); all intermediate values are shown with the same gray level. It is evident that there exists a multiplicity of optimal couples of D and δ which guarantee the achievement of the optimum spectral efficiency, and they may be interpreted as solutions of the system (25). The smallest array diameter for which the optimum spectral efficiency is reached is $D = 0.68\,\mathrm{cm}$, for $\delta = (2n+1)\cdot 30°$, $n = 0, \ldots, 5$. Similarly, there is also a multiplicity of values which cause keyhole conditions to arise. Both optimum solutions and keyholes are distributed on a regular grid, accounting for the effect of the discrete parameter v_{kl}. Anyway, as already explained, choosing a UCA diameter in the range highlighted in Figure 5 will prevent the occurrence of keyhole conditions.

These considerations lead to conclude that a 3-element UCA with a diameter of $68\,\mathrm{cm}$ shows very good performances for a SatCom MIMO system with a carrier frequency of $2.2\,\mathrm{GHz}$, as the achievable spectral efficiency is optimum for some array orientations and shows very little degradation as the receiver changes its position, never collapsing to keyhole values. Nevertheless, this result is based on the empirical observation of the numerically computed spectral efficiency. In the next section we will define a compact index of robustness, which will also allow the comparison between different receiver setups.

B. A General Robustness Index

Besides allowing the validation of the proposed geometrical model for the UCA optimization, the numerical simulation environment also provides a powerful tool to compare different antenna displacements. For a fair comparison between the two architectures under examination, we define now a geometrical parameter s which describes the overall array size as follows:

$$s = \begin{cases} (M_R - 1)\, d & \text{for ULA} \\ D & \text{for UCA} \end{cases}. \tag{26}$$

The spectral efficiency is then in general a function of δ and s. The most desired property is the independence of the spectral efficiency on δ. Therefore, we define the new parameter *Angular Keyhole Sensitivity* as a measure which can be calculated as:

$$\mathrm{AKS}(s) = \sqrt{\frac{1}{2\pi}\int_{-\pi}^{\pi}\left(\frac{C(\delta, s) - \mu_C}{C_{\mathrm{opt}}}\right)^2 d\delta}, \tag{27}$$

where $\mu_C = \frac{1}{2\pi}\int_{-\pi}^{\pi} C(\delta, s)\, d\delta$ is the average spectral efficiency on the whole angular range, and C_{opt} is the optimum theoretical value achievable for the spectral efficiency, according to eq. (5). Moreover, we define

$$C_{\max}(s) = \max_{\delta}\left\{C(\delta, s)\right\}. \tag{28}$$

The general optimization problem for a given array structure in the mobile scenario may be therefore formally expressed as follows:

$$\begin{aligned} s_{\mathrm{opt}} \quad = \quad & \arg\min_{s}\left\{\mathrm{AKS}(s)\right\} \\ & \text{s.t.} \quad C_{\max}(s) \geq \eta \cdot C_{\mathrm{opt}}, \end{aligned} \tag{29}$$

as we try to achieve the maximum independence on the array orientation, but still require that there are some values of δ for which the spectral efficiency is over a certain percentage η (e.g. 95%) of the optimum value.

C. Numerical Optimization

The numerical solution of problem (29) is shown in Figure 7 for a UCA and a ULA of 3 antenna elements. The most restrictive constraint $\eta = 1$ has been considered here. The AKS function is plotted in the upper subfigure and the ratio $C_{\max}(s)/C_{\mathrm{opt}}$ in the lower one. For the ULA, the first minimum of the AKS function (excluding the trivial solution $s = 0$, which does not satisfy the constraint) is located at $s = 1.55\,\mathrm{m}$. For the UCA, the AKS function keeps much lower values in comparison with the ULA (except for $s \simeq 1.2\,\mathrm{m}$, where keyhole conditions arise, as already noticed from Figure 5). The solution of the optimization problem for the UCA is imposed by the constraint, as $C_{\max}$ reaches the optimum value for $s = 0.68\,\mathrm{m}$, which is the same value obtained from the analysis of Figure 6, and is also contained in the desired range

displayed in Figure 5. The length of the optimum ULA would be over 2 times the diameter of the optimum UCA; moreover, the much higher AKS of the ULA denotes anyway worse performances (for ULAs there is always an array orientation resulting in a keyhole).

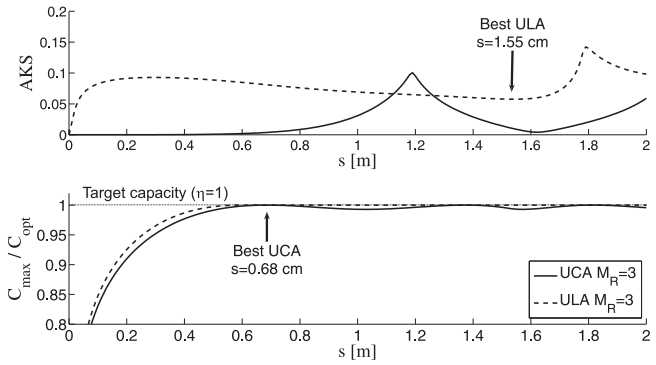

Fig. 7. Angular Keyhole Sensitivity and relative maximum spectral efficiency for a UCA and a ULA of 3 elements.

At last, the optimization problem has been analyzed also for UCAs with $M_R > 3$. Figure 8 shows the AKS function for $M_R = 3, 4, 5$. The plot of $C_{\max}(s)/C_{\text{opt}}$ has been omitted, since it is practically identical to the one shown above for $M_R = 3$, i.e. 100% of the optimum spectral efficiency is reached for $s = 0.68\,\text{m}$ in all three cases. For $M_R = 4$ there are still keyholes arising, as the AKS functions presents two peaks in the considered range. Choosing $M_R = 5$ would actually result in a good keyhole cancellation, but this effect just comes into play for large values of s. The optimum solution for all three cases still stays at $s = 0.68\,\text{m}$; interestingly, the AKS for $M_R = 4$ actually has a local minimum at that point.

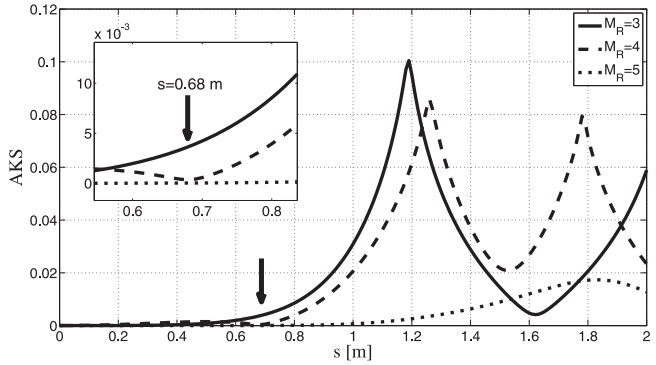

Fig. 8. Angular Keyhole Sensitivity for UCAs with 3, 4 and 5 antenna elements.

D. Summary of Results

The analysis of Figure 8 has shown that the optimum UCA diameter determined for $M_R = 3$ is still optimum also for $M_R = 4$ and $M_R = 5$. Increasing the number of antenna elements actually results in a smaller value of AKS, but the performance achieved by 3 antenna elements might already be sufficient for most practical purposes. In other words, as seen in Figure 5, a very simple triangle-shaped array with optimum diameter would guarantee near-maximum spectral efficiency for any orientation of the receiver, which is not possible with a ULA. Moreover, the resulting array size (below 1 meter) would be compact enough to allow vehicle roof-top installations for S-Band applications.

V. Conclusion

We investigated a MIMO satellite downlink channel between two geostationary satellites and a mobile receiving vehicle on earth, for example a train or a car. The novelty of our approach is based on the derivation of an optimization criterion for UCA antenna arrangements in order to obtain the maximum spectral efficiency. Once the spectral efficiency is optimized for a specific configuration, this optimum value is subject to fades if the terminal is moving. Whereas ULAs are unsuitable because the spectral efficiency can degrade to its minimum value [5], applying UCAs reveals outstanding improvements in terms of the stability of the optimum spectral efficiency in presence of a LOS channel. An example configuration for $M_R = 3$ receive antennae has been presented which guarantees at least 98% of the optimum spectral efficiency durably. With a diameter of only 68 cm in conjunction with a satellite separation of 8° in the orbit, this UCA seems to be very feasible for practical applications for example on the roof top of vehicles.

Appendix

The full expression of the coefficients $G^{(C)}_{kl,m_T}$ and $G^{(S)}_{kl,m_T}$ introduced in section III-E is given below:

$$\begin{aligned} G^{(C)}_{kl,m_T} &= 2\left\{\left[\cos\left(w_{M_R}(k-1)\right)\cos\left(w_{M_R}(l-1)\right)\right]\sin\Delta\theta_{m_T} \right. \\ &\quad \left. + \left[\sin\left(w_{M_R}(k-1)\right)\sin\left(w_{M_R}(l-1)\right)\right]\cos\Delta\theta_{m_T}\sin\phi_R\right\} \end{aligned}$$

$$\begin{aligned} G^{(S)}_{kl,m_T} &= 2\left\{-\left[\sin\left(w_{M_R}(k-1)\right)\sin\left(w_{M_R}(l-1)\right)\right]\sin\Delta\theta_{m_T} \right. \\ &\quad \left. + \left[\cos\left(w_{M_R}(k-1)\right)\cos\left(w_{M_R}(l-1)\right)\right]\cos\Delta\theta_{m_T}\sin\phi_R\right\} \end{aligned}$$

where $w_{M_R} = \frac{2\pi}{M_R}$.

References

[1] I. Telatar, "Capacity of multi-antenna Gaussian channels," *European transactions on telecommunications*, 1999.

[2] P. Driessen and G. Foschini, "On the capacity formula for multiple input-multiple output wireless channels: a geometric interpretation," *IEEE Transactions on Communications*, vol. 47, no. 2, pp. 173–176, Feb 1999.

[3] G. Maral and M. Bousquet, *Satellite communications systems: systems, techniques and technology*. Wiley, 2002.

[4] P. Bøhagen, F. Orten and G. Øien, "Construction and capacity analysis of high-rank line-of-sight MIMO channels," in *Proc. IEEE Wireless Communications & Networking Conference (WCNC) 2005, New Orleans, USA, March 13 - 17*, 2005.

[5] R. Schwarz, A. Knopp, D. Ogermann, C. Hofmann, and B. Lankl, "Optimum-capacity MIMO satellite link for fixed and mobile services," *International ITG Workshop on Smart Antennas, 2008. WSA 2008.*, pp. 209–216, Feb 2008.

[6] ——, "On the prospects of MIMO SatCom systems: The tradeoff between capacity and practical effort," *Systems, Signals and Devices, 2009. SSD '09. 6th International Multi-Conferenceon*, pp. 1–6, March 2009.

[7] R. Schwarz, A. Knopp, and B. Lankl, "The channel capacity of MIMO satellite links in a fading environment: A probabilistic analysis," in *Satellite and Space Communications, 2009. IWSSC 2009. International Workshop on*, 9-11 2009, pp. 78 –82.

[8] A. Abouda, H. El-Sallabi, and S. Haggman, "Impact of antenna array geometry on MIMO channel eigenvalues," in *Personal, Indoor and Mobile Radio Communications, 2005. PIMRC 2005. IEEE 16th International Symposium on*, vol. 1, 11-14 2005, pp. 568 –572.

[9] S. Yan and Z. Yerong, "Maximum MIMO capacity of Rice channel," in *Wireless Communications Signal Processing, 2009. WCSP 2009. International Conference on*, 13-15 2009, pp. 1 –5.

[10] W. Jakes, *Microwave Mobile Communications*. John Wiley & Sons, 1974.

[11] ETSI, "Digital Video Broadcasting (DVB); DVB-SH Implementation Guidelines," European Telecommunications Standards Institute, Tech. Rep. TS 102 584, 2008.